High-resolution quantification of groundwater flux using a heat tracer: laboratory sandbox tests

By

Brant E. Konetchy

Submitted to the graduate degree program in Geology and the Graduate Faculty of the University of Kansas in partial fulfillment of the requirements for the degree of Master of Science.

_____
Co-Chair Gaisheng Liu

_____
Co-Chair Randy L. Stotler

_____
Leigh A. Stearns

Date Defended: August 15, 2014

The Thesis Committee for Brant E. Konetchy

certifies that this is the approved version of the following thesis:

High-resolution quantification of groundwater flux using a heat tracer: laboratory sandbox tests

_____

Co-Chair Gaisheng Liu

_____

Co-Chair Randy L. Stotler

Date approved:

Abstract

Groundwater flux is the most critical factor controlling contaminant transport in aquifers. High-resolution information about groundwater flux and its variability is essential to properly assessing and remediating contamination sites. Recently, we developed a new thermal method that has shown considerable promise for obtaining such information in an efficient fashion. This new approach is based on the previously proven method of using a heat tracer to track groundwater movement and the development of fiber optic distributed temperature sensing (FO-DTS) technology for high-resolution temperature measurement (cable wrapping). Results of an initial field application indicated that heat-induced temperature profiles provided new insights into subsurface flow variations. However, the relation between the thermal profiles and groundwater flux is only qualitative; a quantitative analysis is highly desirable in order to obtain a more definitive relationship between the heating-induced temperature increase and groundwater flux. In this work, we constructed a sandbox to simulate a sand aquifer and performed a series of heat tracer tests under different flow rates. By analyzing the temperature responses among different tests, we developed a quantitative temperature-flux relationship, which can be used for the new thermal approach to directly predict groundwater flux under field conditions. A new method implementing a borehole liner is introduced to separate the two main heat transport mechanisms of advection and thermal conduction by preventing flow from entering the well during heat tests. This method has shown the ability to diagnose if thermal conduction is homogenous or heterogeneous within the tested domain.

Acknowledgments

This work was funded by the NIWR/USGS National Competitive Grant Program (project number 2011KS113G). I would like to thank Steve Knobbe and Ed Reboulet of the Kansas Geological Survey geohydrology section for their help in setting up and designing the sandbox, and continued support through the entire research process. I am grateful to the entire faculty, staff, and fellow students at both the University of Kansas and Kansas Geological Department; my thesis committee members whose guidance and continual support allowed me to improve as a hydrogelogist.

Table of Contents

Introduction

Characterization of groundwater flux is an important step in understanding and evaluating many hydrogeological processes in the subsurface. Determining variations in groundwater flux can lead to a more effective and efficient contaminant site remediation, by gaining the ability to better predict solute transport (Dagan, 1989), and target sections of high mass flux (Suthersan et al., 2010). The ability to characterize groundwater flux at a resolution useful to those ends has proven to be a difficult challenge, as current methods are limited in their ability to resolve small scale variations in groundwater flux.

Alternative groundwater flux estimation tools (e.g, Kerfoot, 1988; Ballard,1996; Hatfield et al., 2004; summary in Bayless et al., 2011) have been developed, but still remain limited in their ability to resolve groundwater flux distribution at a high level of detail (decimeter scale or smaller). However, recent advances in fiber optic distributed temperature sensing (FO-DTS) technology (Selker et al., 2006; Tyler et al., 2009; Suárez et al., 2011), and its increasing use and sophistication when applied to hydrogeologic borehole studies (Hurtig et al., 1994; Förster et al., 1997; Macfarlane et al., 2002; Freifeld, 2008; Leaf et al., 2012), have led to a new a high-resolution groundwater flux characterization (GFC) probe. The GFC probe, developed by the Kansas Geological Survey, has shown the ability to qualitatively delineate variations of groundwater flux within boreholes based on temperature responses (Liu et al., 2013).

The GFC probe uses FO-DTS to record vertical variations in horizontal groundwater flux through active heating of the probe (Liu et al., 2013). The temperature change measured on the probe is primarily controlled by two different heat transport

mechanisms, thermal advection due to groundwater flux around the probe, and thermal conduction between the probe and the surrounding material. Assuming thermal conduction is relatively constant, higher temperature increases indicate lower flux zones, while lower temperature increases indicate higher flux zones (Liu et al., 2013; Fig.1).

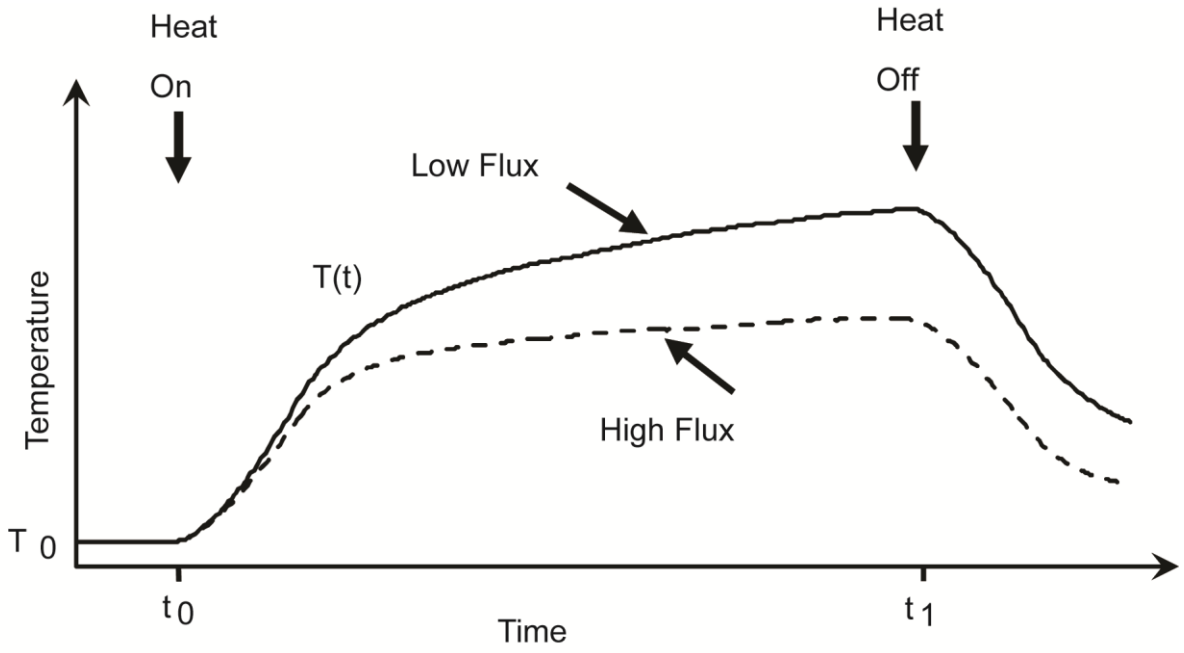

Figure 1. Heat-induced temperature increase at different groundwater flux rates assuming a constant rate of thermal conduction (Liu et al., 2013).

To fully utilize the GFC probe, the relationship between groundwater flux and temperature response needs to be established. The current approach does not provide direct measurement of groundwater flux values, but instead qualitative estimates based on analysis of heat-induced temperature responses. In this study, using a laboratory setting in which the groundwater flux can be controlled within an artificial confined aquifer, temperature responses are correlated with various groundwater flux values. This approach allows for the relationship between the two terms to be developed, so

that the GFC probe can be used to quantitatively determine groundwater flux values based on temperature responses under applicable conditions in the field.

Background

Groundwater Flux

Groundwater flux is the amount of water discharged through a unit area expressed in units of velocity, which is also known as Darcy velocity (Freeze and Cherry, 1979; Fetter, 2001). Groundwater flux is most readily estimated by using Darcy's law, $q = k \times i$, where q is the Darcy velocity, k is the hydraulic conductivity, and *i* is the hydraulic gradient. In order to calculate Darcy velocity at least three wells are needed to measure water levels to calculate *i*, and hydraulic tests are used to estimate k. In a laboratory setting using a sandbox set-up, Darcy velocity can be directly calculated from the total discharge rate, $q = Q/A$, where Q is the total discharge that can be measured by a flowmeter, and A is the cross-sectional area through which the water flows. Laboratory experiments allow for the discharge rate to be monitored, and setting up a confined aquifer setting ensures that all flow is through the cross-sectional area of the sandbox. Under field conditions, groundwater flux determined from Darcy's law is generally averaged over a large volume giving a general description of flux (Freeze and Cherry, 1979). This general description of flux is not at the detail or resolution needed for better site remediation and characterization (Liu et al., 2013).

Alternative methods to measure groundwater flux have been developed to overcome this lack of resolution. The tools developed are all generally installed within a borehole, and use some form of a tracer to estimate groundwater flux. The basic

principle behind these estimations is that the tracer is primarily transported by groundwater flow; by monitoring how the tracer moves, groundwater flow can be estimated. The tracer used, and how it is monitored are the key differences between different methods. The following alternative methods illustrate the variety and degree to which the problem of groundwater flux estimation has been addressed over the last 25 years. The heatpulse flowmeter uses a series of thermistors surrounding a heat source to determine the magnitude and direction of groundwater flow (Kerfoot, 1988) In this approach, thermistors record the arrival and decay of the heat pulse emitted from the center source. Depending on which thermistors pick up heat, the direction of flow can be determined, while the time it takes for the heat pulse to arrive and dissipate determines the flow rate. The In Situ Permeable Flow Sensor also uses heat as means to calculate groundwater flow and direction (Ballard, 1996). The sensor is buried in direct contact with the porous media, and heated over the entire length of the cylindrical body. As groundwater flow passes around the probe, areas will become cooler or hotter depending on the direction and magnitude of the flow (Ballard, 1996). The acoustic Doppler velocimeter uses acoustic signals to track particles that flow through the well (Wilson et al., 2001). The probe uses the acoustic signals to create three dimensional measurements of the particles path, which are directly converted into groundwater flux in the borehole. The colloidal borescope flowmeter uses a camera system to visually track particles passing through the well due to groundwater flow (Wilson et al., 2001). As the naturally buoyant colloids pass through the well they are tracked and digitized so that they can be easily processed using a computer algorithm to calculate their speed and direction. The fluid-conductivity logging system displaces natural

groundwater with deionized water, and then conducts a series of temperature and electrical conductivity profiles to determine locations of water entering and leaving the system (Tsang et al., 1990; Pedler et al., 1995). This method uses time series of electrical conductivity data to determine flow rates. It can also survey the entire borehole, but cannot determine flow direction (Wilson et al., 2001; Bayless et al., 2011). The passive flux meter uses a sorbent material that has its matrix filled with water soluble tracer (Hatfield et al., 2004). As the tracer dissolves into the groundwater, the rate at which that occurs is proportional to groundwater flux, making the term possible to calculate. The probe also serves a dual purpose of absorbing contaminants. The rate of contaminant absorption can be used to calculate contaminant flux. The point velocity probe uses a saline tracer around a cylindrical body to estimate groundwater velocity (Labaky et al., 2007). As the saline tracer moves around the probe it contacts a detector that can pick up electrical conductance changes in the water, which is used to calculate the tracer travel time and thus groundwater flow rate (Labaky et al., 2007). The probe has shown the ability to detect cm-scale variations in groundwater flow, and can be used to create a continuous profile, but over series of days to weeks (Labakey et al., 2007; Labaky et al., 2009). The probe is installed into the subsurface so that it is in direct contact with the porous media.

It is evident that there are multiple methods that can be used to estimate groundwater flux, and each comes with its own limitations and benefits. However, the main drawback with most of these devices is the inability to create a continuous borehole profile at a high resolution that is often needed in contaminant site remediation, or those that can do so at only a few points or over a large period of time.

This creates a choice between a high resolution device over a discrete area, or less resolution over a larger area. The choice of which probe to use or more importantly at which interval to monitor with the probe becomes a critical factor, as preferential flow paths or barriers may easily be missed (Liu et al., 2013). The GFC probe addresses this issue by producing a continuous borehole profile at high-resolution detail within a single day of fieldwork (Liu et al., 2013).

Distributed Temperature Sensing

Distributed Temperature Sensor (DTS) technology consists of two parts, a DTS instrument (Sensornet Sentinel) and a fiber optic (FO) cable, and can allow for near continuous spatial (meter resolution) and temporal (minutes) temperature datasets (Selker et al., 2006; Tyler et al., 2009, Suárez et al., 2011). The Sensornet Sentinel regulates a laser pulse through the DTS-FO cable and records the photon backscatter used to calculate temperature and travel time to determine temperature measurement location along the cable. DTS technology is based on Raman backscatter, which is induced along the FO cable when incident light encounters matter, is absorbed and reemitted at a different wavelength (Selker et al., 2006; Tyler et al., 2009, Suárez et al., 2011). When the wavelength frequency shift is higher than the incident light, it is referred to as anti-stokes backscatter, and when the frequency shift is lower it is called stokes backscatter (Selker et al., 2006; Tyler et al., 2009, Suárez et al., 2011). The Sensornet system records these Raman backscatter photons, and uses the ratio of anti-stokes to stokes backscatters to determine the temperature. Temperature can be determined by this ratio due to anti-stokes backscatter being dependent on both the

intensity of illumination and the temperature at that location, whereas stokes backscatter is dependent primarily on the intensity of illumination only (Selker et al., 2006).

DTS temperature resolution depends on the desired spatial resolution, and time period over which photons will be collected. Lower spatial resolution allows for larger quantities of photons to be collected over a longer cable, allowing for a better convergence on the temperature, but will lack any useful temperature changes over smaller intervals. Higher spatial resolution will give better insight into temperature changes over small distances, but will not have as many photons to accurately determine the temperature, lowering the quality of the data. The longer the collection period, the better quality temperature data, as more photons can be collected. However, like spatial resolution, collection period depends on the criteria of the experiment as to what time to choose. Longer time periods allow for better data collection, but do not allow temperature changes to be seen over smaller time intervals.

DTS-FO cables can collect data as a single ended cable or as a double-ended cable by connecting the cable back to the instrument. Single-ended cable applications are best used when little to no stress is applied to the DTS-FO cable (bent, sliced, stretched, etc.) as the differential attenuation within the cable is minimal (Selker et al., 2006; Tyler et al., 2009, Suárez et al., 2011). The GFC probe in this study uses double-ended measurement due to the wrapping of the cable. Differential attenuation is the measure of the different absorption rates of stokes and anti-stokes along the path of the cable, these different rates can cause erroneous temperature measurements (van de Giesen et al., 2012). To correct for differential attenuation in the double-ended

measurement process, a laser pulse is sent in the forward direction for half of the total collection period, and then in the reverse direction for the other half of the collection period. In this way, two temperature measurements can be taken for a single location, one in the forward direction and the other in the reverse direction, allowing for differential attenuation to be calculated and corrected, improving the quality of the data (Tyler et al., 2009; van de Giesen et al., 2012)

Heat as a Groundwater Tracer

Heat as a groundwater tracer in hydrogeology first began in the 1960's and has recently gained more traction as a hydrogeologic tool as technology has increased to allow for better temperature measurements (Anderson, 2005; Rau et al., 2014). The principle idea behind using heat as a tracer is to be able to track groundwater flow paths and rates by monitoring temperature variations both natural and induced, as an alternative to measuring head values or to help support head measurements (Anderson, 2005). It is a relatively cheap and easy method to supply and monitor heat, as well as avoiding any concerns that are inherent when using other tracer methods, such as radioactive or chemical. The main transport mechanism by which heat is moved through the subsurface is that of thermal advection (also known as convection) and thermal conduction (Anderson, 2004; Rau et al., 2014). Thermal conduction is when heat is transferred from one material to another through diffusion and collision of microscopic particles in the presence of a temperature gradient, with higher thermal conduction allowing for heat to more readily move through material. The higher the temperature gradient, the more heat that will be transferred, and vice-versa. The

complexity with thermal conduction in aquifer settings is that the heat travels through two mediums, the aquifer matrix (rock or unconsolidated sediments) as well as the groundwater. Both thermal conductivities (water and rock) must be considered when trying to calculate heat conduction, but is generally averaged together over a significant enough volume to produce a bulk conductivity value (Anderson, 2005; Rau et al., 2013).

Thermal advection is the transport of heat due to flowing groundwater. Two different types of advection can occur, free advection which is driven by temperature induced density differences, or forced advection in which heat is transported by flowing groundwater without buoyancy effects (Anderson, 2005). The heat transport equation used to model how heat moves in aquifers is analogous to the advection-dispersion equation, with thermal conduction similar to the dispersion term, and thermal convection analogous to the advection term (Anderson, 2005). The focus of this study is on the thermal advection transport mechanism, and how varying the discharge rate, and thus the advection rate, will affect the temperature response produced by the GFC probe.

Most current research focuses on using heat as a means to better understand surface and groundwater interaction (e.g. Lowry et al., 2007; Westhoff et al., 2007; Vogt et al., 2009; Schuetz and Weiler, 2011), while other studies have incorporated heat as means to track hydrogeologic process in borehole studies (Hurtig et al., 1994; Förster et al., 1997; Macfarlane et al., 2002; Freifeld, 2008; Leaf et al., 2012). This type of research has readily adopted the use of DTS as a means to thoroughly and accurately record temperature fluctuations (Suárez et al., 2011). Both surface-groundwater and borehole studies have shown ambient temperature fluctuations can be as a means to obtain groundwater flux estimations, or active heating to act as the tracer. Cases in

which heat is actively applied in borehole studies are most comparable to the way in which the GFC probe operates in this study. One of the first uses of the DTS and active heating in borehole studies was performed by Hurtig et al. (1994). This study monitored temperature variations within a borehole in Switzerland's Grimsel Test Site, as hot and cold water were injected. They were able to show the existence of a fracture as the temperature profile showed sudden drop in temperature. The highly transmissive fracture explained the rapid loss of the heated water, and thus the cooler temperature response. Macfarlane et al. (2002) performed a heat tracer test by injecting heated water into a well, while pumping a nearby well within the Dakota aquifer in western Kansas. In both wells DTS was used to monitor the temperature using a double-ended set-up to improve temperature resolution. The results of the temperature profiles showed a local heterogeneity of higher hydraulic conductivity within the upper part of the Dakota aquifer. Freifeld et al. (2008) used thermal perturbation to estimate thermal conductivity in a borehole. They actively heated the borehole and recorded the response using DTS; a resistance heating cable was used rather than injecting heated water. By observing the heat dissipation after a long heating interval, the thermal conductivities of the borehole were estimated. Becker and Hawkins (2012) used wrapped DTS probe to monitor actively heated temperature response through a series of injection wells. The wrapped DTS probe was used to enhance the resolution along the probe, and the injected heat as a means to monitor heat transport through a heterogeneous system. They found that fractures significantly affected the flow, and that groundwater tended to form channelized flow along these fractures.

These studies shows the progression of heated borehole studies using DTS, as well as the individual elements that helped to develop the GFC probe including wrapped cable to improve vertical resolution, and resistance heating cable instead of fluid injection to introduce heat.

Sandbox Tracer Experiments

The use of a laboratory sandbox in hydrogeologic studies is prominent and invaluable as a means to study flow and transport. Sandboxes can provide a control setting to study the physical and chemical processes that may be difficult to determine or control within a field setting (Silliman et al., 1998; Fernàndez-Garcia et al., 2004; Close et al., 2008). In tracer studies sandboxes have proven to be a reliable means to test and further evaluate how material is transferred within an aquifer (Silliman et al., 1998; Barth et al., 2001; Fernàndez-Garcia et al., 2004; Jose and Rahman, 2004; Close et al., 2008). Groundwater flux estimation tools have also taken advantage of using sandboxes when evaluating or calibrating their tools and methods (Hatfield et al., 2004; Labaky et al., 2007; Gauaraglia et al., 2008; Bayless et al., 2011). The scale of sandboxes used in various experiments ranges generally from small scale desktop set-ups (e.g. Danquigny et al., 2004; Labaky et al., 2007; Gauaraglia et al., 2008; Bowen et al., 2012) to large scale set-ups requiring large or dedicated space (e.g. Fernàndez-Garcia et al., 2004; Jose and Rahman, 2004; Liu et al., 2007; Close et al., 2008; Bayless et al., 2011). The size of the sandbox depends on the type of experiments performed and the tools and equipment used during those experiments. In this research a large-scale sandbox was chosen as it gave enough distance between the

probe and sandbox walls so that boundary conditions would not be a problem, as well as enough height to obtain a large sample size along the GFC probe. The main reason a laboratory sandbox setting was chosen was the ability to control the flow rate, allowing for the relationship between flow rate and temperature response to be observed.

The experiments performed by Gauaraglia et al. (2008) are most analogous to the experiments performed in this research. They used a sandbox laboratory setting in which various flow tests were performed on the heatpulse flowmeter. The sandbox consisted of a cylindrical tank that contained larger porosity gravel overlain by homogeneous sand overlain by another gravel layer, and water was flowed vertically through the tank. They found that the heat pulse probe had an upward limit of 70 m/d at which the probe could no longer determine the actual flow rate within the sandbox. The experimental set-up used in this research is much the same, as is the overall mechanism used by both probes to estimate groundwater flux (heat). The main differences are the sandbox construction and the technology used by each probe. The Gauaraglia et al. (2008) sandbox was much smaller in scale, as the heatpulse flowmeter does not require a large area to make measurements. While more convenient for sandbox experiments, this also reveals the discrete measurement interval of the device that the GFC probe addresses with its larger measurement window. It is the size of the GFC probe that drives the need for a large-scale sandbox so that the probe can be properly evaluated.

Methods

Groundwater Flux Characterization Probe

Combining the continuous spatial and temporal resolution provided by the FO-DTS cable (Selker et al., 2006; Tyler et al., 2009, Suárez et al., 2011), along with heat as a groundwater tracer (e.g. Anderson, 2005; Rau et al., 2013), high-resolution groundwater flux intervals can be determined through heating-induced temperature response (Liu et al., 2013). Groundwater flux can be determined by the magnitude of overall temperature change recorded by the GFC probe in the presence of groundwater flow.

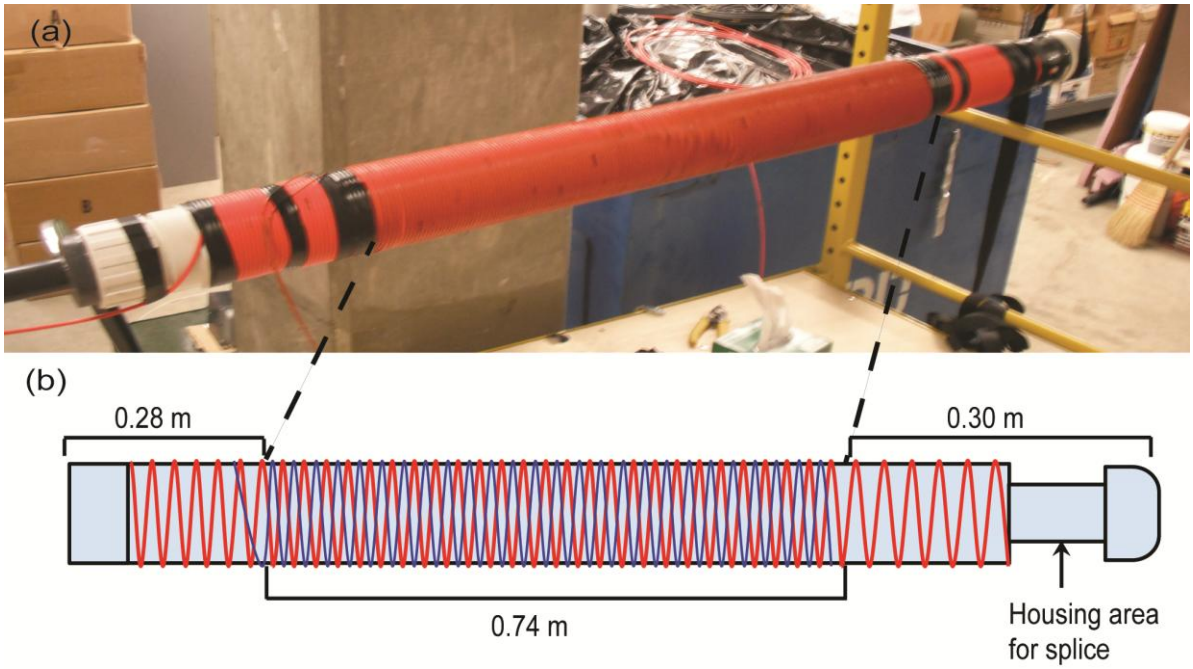

Figure 2. Lab GFC Probe. (a) Image of complete GFC probe tested in the lab. Red cable is FO-DTS cable. Orange cable is heating cable. (b) Schematic of GFC probe. Red lines represent FO-DTS cable, blue lines represent heating cable.

The GFC probe we constructed by wrapping FO-DTS cable and a heating cable around a hollow pvc (polyvinyl chloride) pipe (Fig. 2).

The FO-DTS cable (AFL LSZH FD-3690) is composed of two fiber cores housed

in a single jacket. The FO-DTS cable has a total of three splices in order to run double-ended measurements (van de Giesen et al., 2012), two at the top for the forward and reverse directions, and one at the bottom of the probe to connect the two fibers. The FO-DTS cable is connected to the Sensornet Sentinel which regulates the laser pulse through the cable, and records the resulting photon backscatter. The Sensornet Sentinel has a sampling resolution of 1 meter over a 1 minute. When the cable is wrapped, as done in the GFC probe, the vertical resolution of temperature measurements can be improved to just a few centimeters (Vogt et al., 2010; Liu et al., 2013). Wrapped around the FO-DTS cable is a heating element, a vinyl-coated stainless steel wire rope that is connected to a variable-output transformer to allow for active heating of the probe. The heating cable is wrapped in between the grooves of the FO-DTS cable (Fig. 2).

The GFC probe used in the lab flow experiments has a similar build to the probe created in Liu et al., (2013). However, it has been slightly modified and scaled down to allow a better fit with the lab flow setup. The main difference is that the probe and wrapped section are about ¼ the size of the original field probe, and the bottom section has been modified by removing the original k-packer and replacing it with a sealed cap to increase the length of the measurement interval. A total of 208 meters of FO-DTS cable was used in the construction of the probe, temperature calibration baths, and connections to the Sensornet Sentinel. The main probe body (area wrapped with heating cable) is composed of 55 m of wrapped FO-DTS cable over a 0.74 m length, producing a vertical resolution of 1.48 cm per temperature measurement (Fig. 2). The Sensornet Sentinel was set up to record temperatures at every meter and over a 1 min

collection period in a double-ended measurement mode, 30 seconds in the forward direction and 30 seconds in the reverse direction.

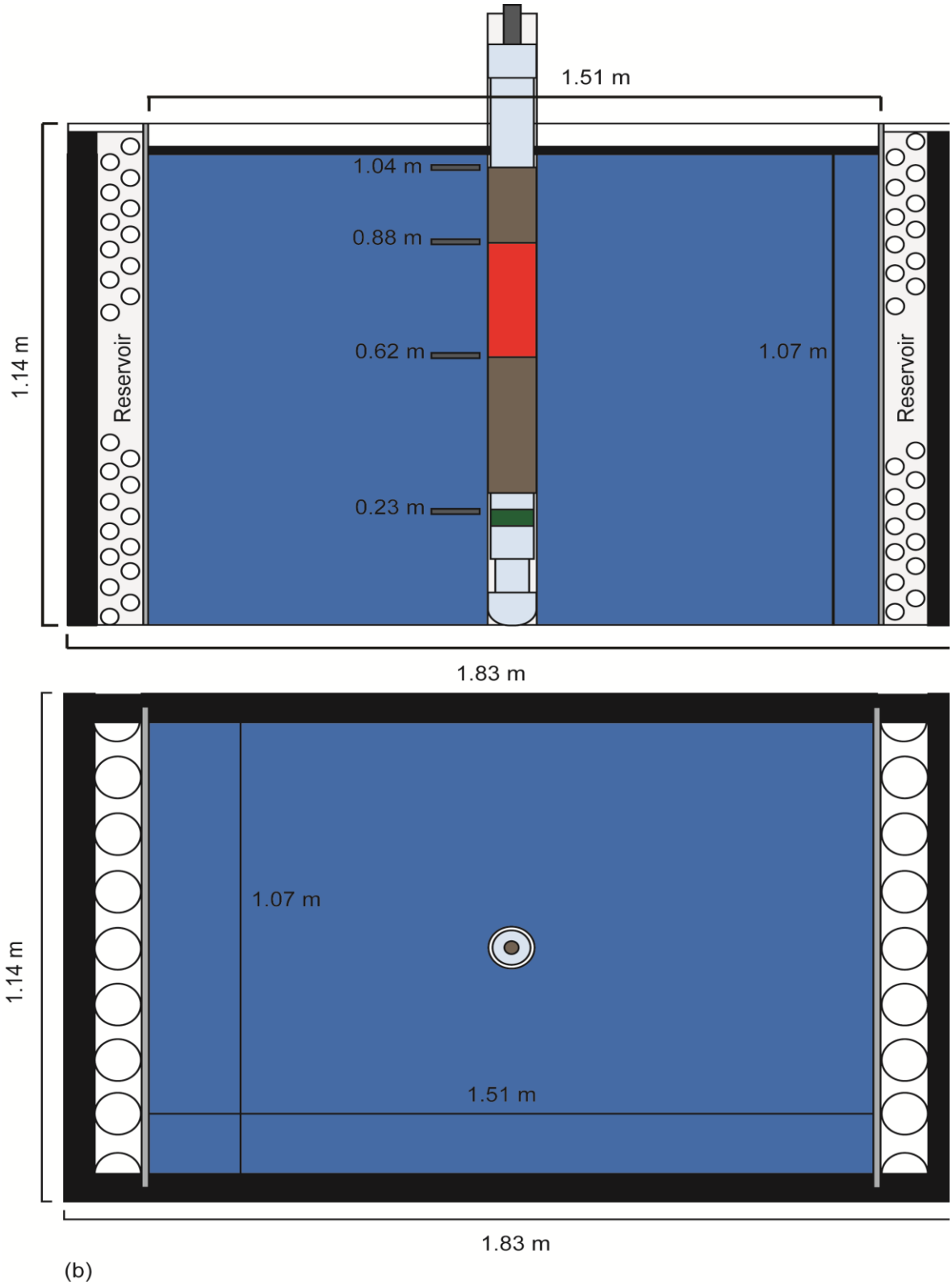

Figure 3. Schematic of sandbox. (a) Cross-sectional view of sandbox with GFC probe. Red section indicates the interval over which the individual temperature measurements were spatially averaged to produce one average value per measurement time. Green section represents the interval over which the background temperature was obtained. Grey section represents area on probe that is actively heated (including the red). Black represents foam insulation boards. Light grey section represents perforated pvc that acts as the main screen to hold back the sand from entering the reservoir while still allowing water to freely flow between. (b) Top view of sandbox schematic.

Sandbox

A steel container was used to construct the sandbox for testing the GFC probe (Fig. 3). The inside of the container was cleaned and a two-part epoxy coating was applied to prevent rusting and the growth of biomass. A 11.47 cm diameter, 5.08 cm high pvc flange was installed at the center of the bottom of the container, to act as an anchor for the well. Rigid foam insulation boards were installed inside of the container to minimize the impacts of room temperature variations and the highly conductive steel frame on the sand aquifer during the tests. Specifically, the inside walls of the box were covered in 3.81 cm thick rigid foam boards and the bottom of the box was covered by a 1.91 cm thick foam board. A hole was cut into the bottom foam piece to allow it to sit around the pvc flange. A 1.3 m long, 10 slot, 10.2 cm diameter pvc well was then glued into the flange.

In order to maintain two reservoirs within the container, sixteen 10.2-cm diameter pvc pipes were used as space retainers. Eight pvc pipes were used for each reservoir, 7 whole pipes and 1 pipe cut lengthwise in halves (Fig. 3). The two half pieces were installed 1.27 cm into the side insulation foam boards, to lend additional support to the reservoir walls. All pvc pipes had 3.81 cm diameter holes drilled throughout the pipe to ensure free flow within the reservoir, while also maintaining the structural strength of the pvc pipe. The reservoir walls consisted of a 0.64 cm-thick perforated pvc screen with hole diameters of 1.27 cm and a fine grained moisture resistant polyester mesh. The perforated pvc screen was used to provide the structural support for the walls, and retained the majority of the sands from entering the reservoirs. The polyester mesh covered the perforated pvc screen, preventing any fine grained materials from passing

through the holes in the pvc screen. Recesses of 1.27 cm were etched into the surrounding foam insulation boards, and the pvc screen was installed into the recesses with glue. A silicone caulk was applied around the screen to prevent the sand from passing around or under the screen.

Commercial medium grade sand (Quikrete, Medium No. 1962, #20 - #50, 0.8-0.3 mm) was used for the synthetic aquifer, and wet packed into the container (Fernández-Garcia et al., 2004; Jose et al., 2004). The container was initially filled with water ¼ of the way, and then 80 lbs bags of sand were added to the box and manually mixed to allow for even distribution. This process was repeated until more water was needed to keep a water level above the sand at all times.

Once the sand reached a height of (1.07 m), it was smoothed at the top to create a flat surface on which a confining rigid foam board was placed. A 0.64 cm-thick foam board was installed on top of the sand to act as a confining unit, and to also help further insulate thermally the sand aquifer. On top of the confining unit, bags of sand were placed evenly around to add weight and keep the foam board from rising. A silicone caulk was applied along the edges to prevent water from flowing up.

After the sandbox was constructed, Darcy's flow experiments showed that the average hydraulic conductivity of the aquifer was 218 m/d in the horizontal direction. Sample analysis indicated the sand had a total porosity of 36% and effective porosity of 33%.

Data Analysis

Processing of raw temperature data was performed through the methods outlined in van de Giesen et al. (2012). The data points used in calculating the temperature response were at some distance away from both ends of the probe to minimize the boundary impacts of the box and probe (Fig. 3), which consisted of 21 m of wrapped cable (i.e., 21 data points). These points were spatially averaged to compute probe temperature responses during heating. Temperature response (delta T) values are calculated using,

$$\Delta T_{ave} = \frac{1}{t_1 - t_0} \int_{t_0}^{t_1} [T(t) - T_0] dt, \quad (1)$$

where T_0 is the temperature at time t_0 before heating is started, and T(t) is temperature at time t_1 when heating ceases (Liu et al., 2013). However, due to temperature fluctuations in the room, the background temperature in the sand box does not remain stable through the heating test. In order to correct for this, the DTS-measured temperature along a 5.92-cm interval at the bottom of the probe (Fig. 3), which was 0.39 cm below the bottom of heating section, was used as the background temperature throughout the test. The correction of background temperature variation was achieved by subtracting the background temperatures from the probe temperatures for each time step (Fig. 4).

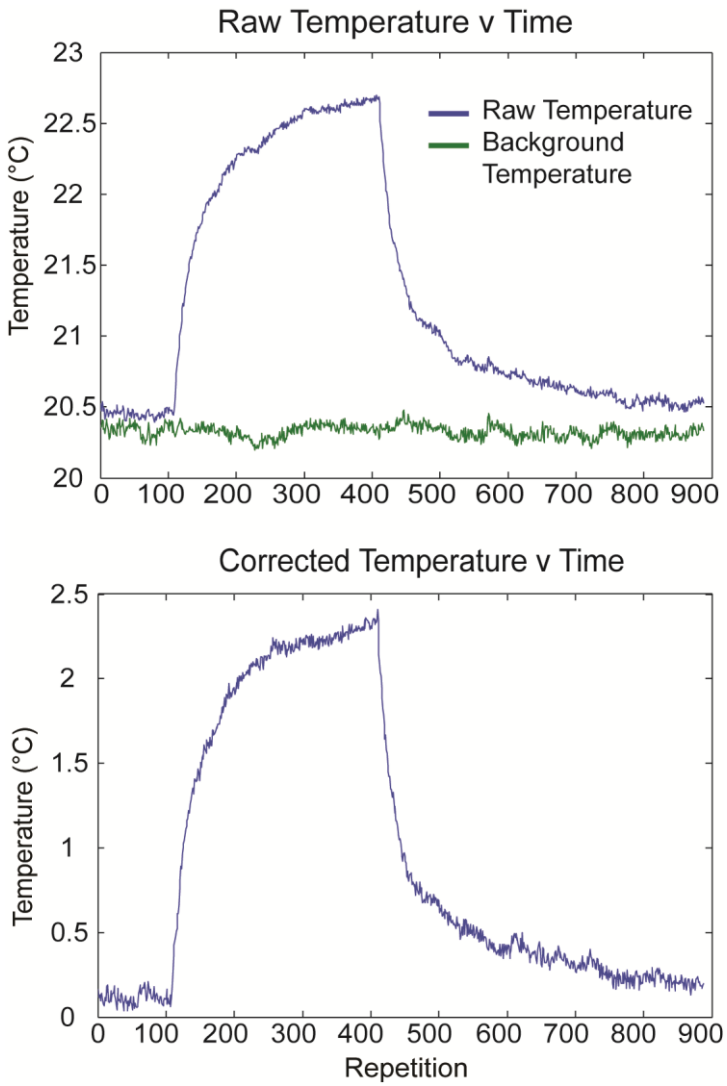

Figure 4. Representative 5 hour heating test for a no flow test. Top plot shows raw and background temperature through time (each repetition is about 1 min). The bottom plot shows the corrected probe temperature after subtracting the background

Once the background temperature correction was made, equation 1 was applied to the corrected data to calculate the delta T value for a given flux rate. In these experiments, T_0 is averaged over a 1 hour period before the start of the heating test. The average temperature for the heating test is calculated by averaging over the heating test length (i.e. t_1 = 5 or 10 hour period). The error of the temperature measurement is based on the root mean square error (RMSE) using temperature

probes connected to the Sensornet Sentinel as the true temperature response, and the FO-DTS cable temperature readings located within the calibration baths as the measured values (van de Giesen, 2012). We assume that the temperature error in the baths is the same for all measurements along the cable.

Lab Flow and Heating Tests Set Up

The GFC probe was secured into the well by running a rope around the box and on top of the probe, instead of using a K-packer on the bottom of the probe as in the field. This method was chosen in order to prevent the well from being pulled from the bottom of the sandbox when the probe was moved using the K-packer. The calibration baths consisted of a cooled and heated bath, which were maintained by adding ice and installing an aquarium heater, and contained 33 m and 32 m of FO-DTS cable, respectively (Hausner et al., 2011; van de Giesen et al., 2012; Liu et al., 2013). The groundwater flux in the sandbox is controlled by using a peristaltic pump to remove water from the lower reservoir to the upper reservoir at a constant rate (Fig. 5).

The flow rate, Q, was monitored through a flow meter with a range of 200 to 2000 ml/min. The Darcy's velocity was calculated as $q = Q/A$, where A was the cross-section area of the confined aquifer. Water levels were maintained above the confining unit during all tests to ensure confined flow. A variable-output transformer was used to control the power output (heating) along the heating cable. A manometer was installed to measure the hydraulic gradient during each flow test (Kelly and Murdoch, 2003).

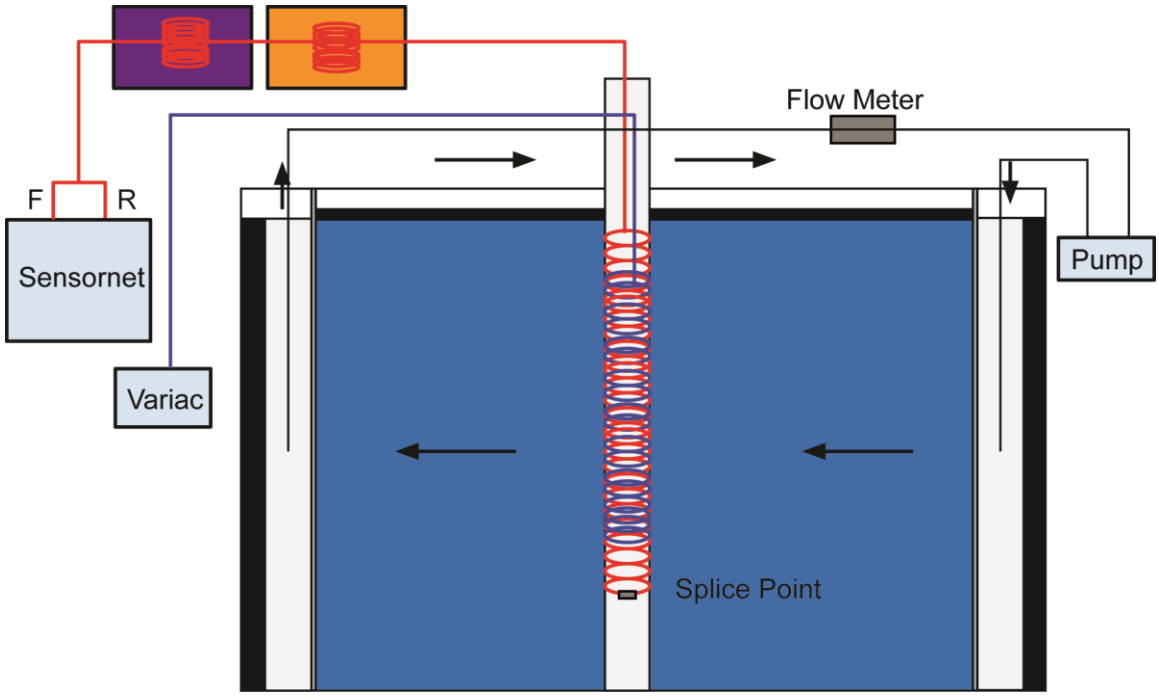

Figure 5. Schematic of laboratory set-up. F represents the forward direction and splice point, and R represents the reverse direction and splice point. The purple box represents the cooled calibration bath and the orange box the heated calibration bath. The arrows represent flow direction in the sandbox and through the plastic tubing.

Experiments

Three experiments were performed to determine the quantitative relationship between groundwater flux and temperature change.

1. The first experiment used a short term heating interval as performed in Liu et al. (2013). The probe was heated at a constant power output of 8 W over a five hour period. The flow rate was varied from 0 to 1000 ml/min (Darcy's velocity 0 to 1.28 m/d), and increased by an interval of 100 ml/min. A flow rate of 100 ml/min was not used as it was outside of the flow meter range. Pumping began 1 hour before heat was turned on to create a steady flow field. The purpose of these experiments was to determine temperature responses that were similar to

those in the previous short-term field tests.

2. The second experiment involved a longer heating interval of 10 hours, flow rates were between 0 and 1000 ml/min, but increased at an interval of 200 ml/min. The purpose of these tests was to explore whether temperature signals could be improved by increasing the heating interval from 5 to 10 hours.
3. The third experiment was conducted the same as the second experiment, but with a FLUTe borehole liner installed over the probe (closed well). The liner was first installed into the well and filled with water, forcing the liner against the well so that water could not flow into the well during the flow tests. The probe was then installed into the well with the liner already in place. The purpose of these experiments was to separate the advection from the thermal conduction during the heating tests.

Results

There are a total of 23 temperature points collected for experiment 1, and 11 temperature points collected for experiment 2 that spreads over two distinct time periods (5 in the first period, 6 in the second period). Experiment 3 had a total of 6 temperature points.

In order to facilitate further discussion between the experiments, experiments 1 (blue) and 2 first period (green) are plotted on the same plot (Fig. 6). While experiment 2 second period (purple) is plotted with experiment 3 (red) (Fig. 7). A linear fit was used to describe the relationship between temperature response and Darcy velocity when the velocity was greater than 0.25 m/d (Q 200 mL/min) (Fig. 6,7). Experiment 1 dataset

shows that a linear fit describes the relationship between temperature response and Darcy velocity well with a high R-squared correlation coefficient value of 0.91 and a slope of -0.76 (Fig. 6). Experiment 2 first period dataset also shows a high R-squared correlation coefficient value of 0.99 for the linear trend between temperature response and Darcy velocity and a slope of -1.01 (Fig. 6). Experiment 2 second period slope for the linear trend between temperature and Darcy velocity is -0.72, and experiment 3's slope is 0.0013 (Fig. 7).

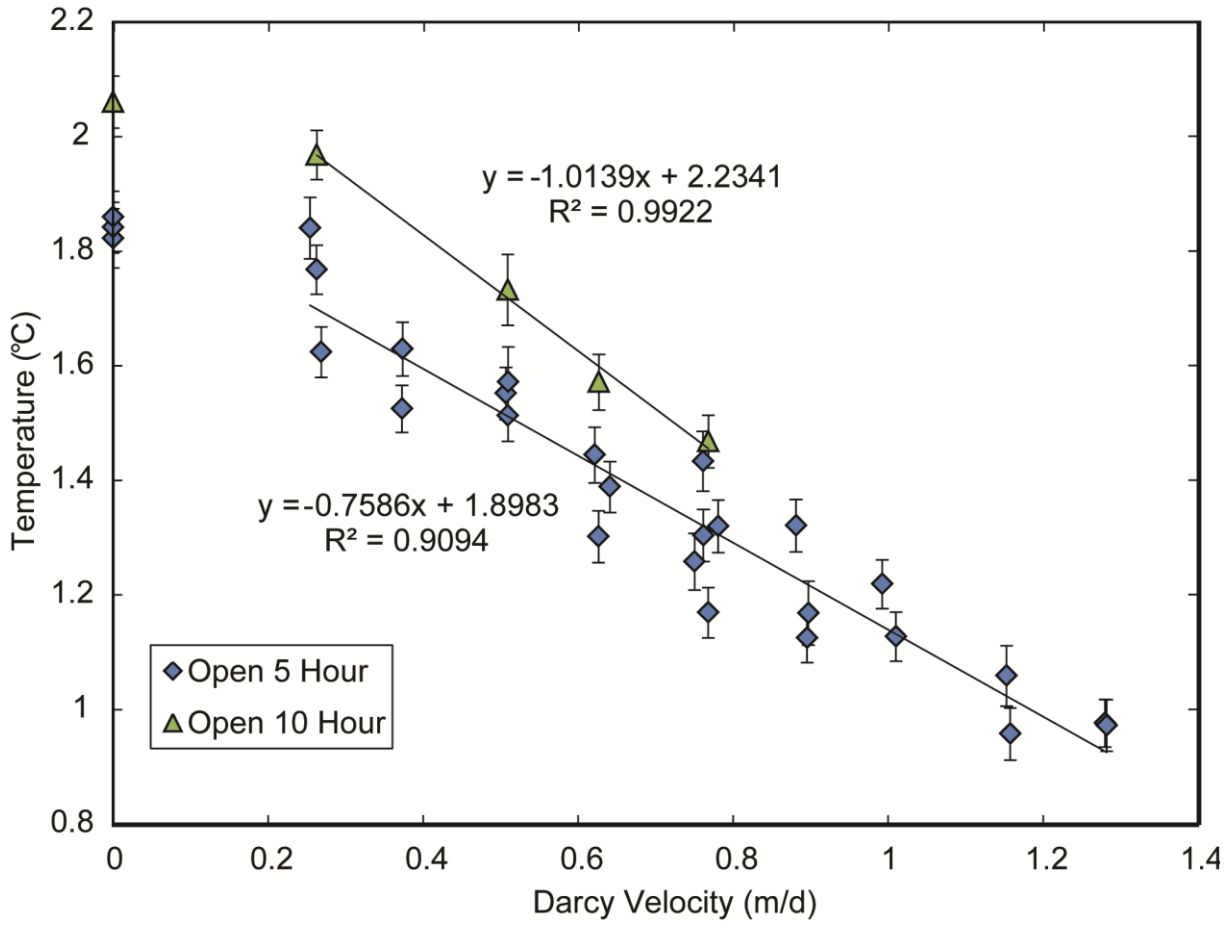

Figure 6. Plot of 5 hour and 10 hour temperature responses versus the average Darcy velocities. The 5-hour data set includes the 23 temperature points collected for experiment 1 and 5 temperature points from experiment 2 that were processed for the first 5 hours. The average standard deviation for the velocity measurements is 0.01 m/d.

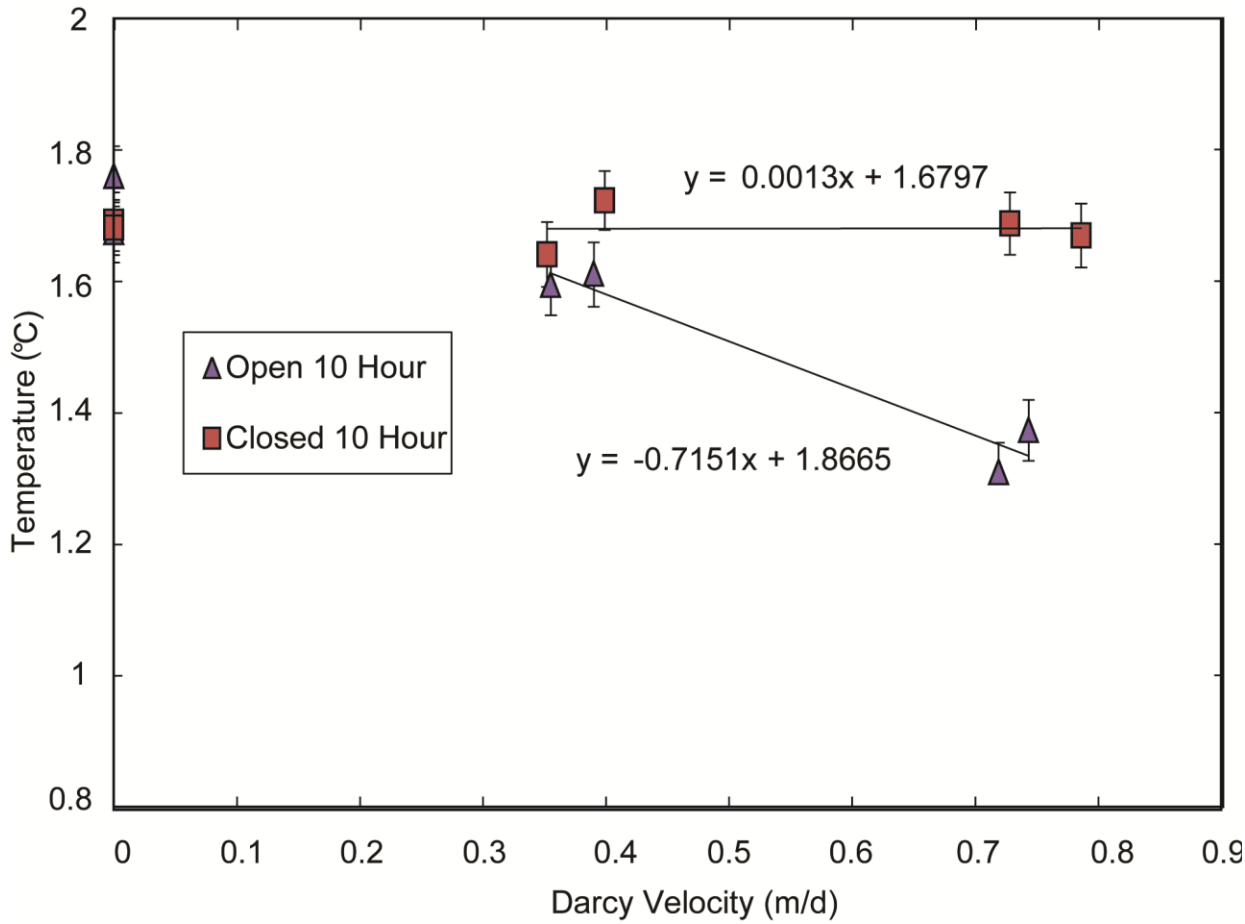

Figure 7. Plot of 10 hour open-well and 10 hour closed-well heating tests. Darcy velocities are for the average values over the entire heating test, with an average standard deviation of 0.02 m/d.

Discussion

Between zero flow and Darcy velocity of 0.25 m/d, there is apparently a break in the linear relation between heating-induced temperature change and groundwater flow rates (Fig. 6,7). This is because as the flux decreases, the role of thermal conduction in the overall heat transport becomes more significant. When thermal conduction dominates the heat transport during the GFC heating test, the temperature change is not sensitive to groundwater flux and the linear function between them at large flux rates

does not remain valid. Further work is needed to better quantify the transition from the advection-dominated heat transport, where the temperature responds linearly to groundwater flux, to the conduction-dominated heat transport where the temperature becomes much less sensitive to flux (where their relation might take on a nonlinear form).

The current GFC probe has difficulties measuring temperature response accurately at a Darcy's velocity less than 0.25 m/d in the 5 hour heating tests. Figure 6 shows that the difference in the 5-hour temperature change is small between velocity 0.25 m/d and no flow, possibly approaching the range of the GFC probe noise. If the GFC probe cannot discern low groundwater flux values (< 0.25 m/d), then only a range of groundwater flux values (0-0.25 m/d) can be assigned to those temperature responses. In cases where higher groundwater flux values exist (> 0.25 m/d) along with lower groundwater flux values (< 0.25 m/d), then GFC probe can still locate the sections of highest groundwater flux. However, if the site is dominated by lower groundwater flux values (< 0.25 m/d), then the GFC probe would be unable to accurately determine higher or lower groundwater flux values.

In order to improve the temperature signal (this will be more critical for the lower velocities, < 0.37 m/d), a longer heating test interval is explored. A longer test time will increase the area under the temperature vs. time curve (Equation 1 and Fig. 4), increasing the time that the temperature responses are driven by advection. A comparison between the 5 and 10 hour heating tests shows the potential of this approach (Fig. 6). The 10 hour dataset shows a larger temperature increase than that for the 5 hour tests at each groundwater flux rate. Due to the longer measurement time,

the time-averaged temperature for 10 hour tests appears to have less noise, and shows more consistently that the heating-inducted temperature increase becomes smaller with the increasing flux rate. Further work is needed to expand the 10-hour data set by running more 10-hour heating tests over a larger range of flux values, to confirm the improved sensitivity of temperature responses to groundwater flux.

The results of the new closed-well method (the third experiment) to potentially evaluate the difference between thermal conduction and advection using the GFC probe can be seen in figure 7. This plot shows a series of open-well (i.e., the well screen is open and water can enter the well) 10 hour heating tests and closed-well (or lined, the well screen is blocked by the sleeve and water cannot enter the well) 10 hour tests. For the closed well data, the slope is much smaller (0.0013), indicating that flow is not entering the well and lowering the temperature response, causing little difference in the heating responses between different flow rates. Note that the open and closed datasets have very close temperature responses at no-flow, indicating that adding the sleeve has not changed the thermal properties of the probe. This is important as the purpose of adding the liner is to create a no-flow condition in the well, while minimizing any significant impact to the thermal conduction property of the tested domain. Because the no-flow temperature responses are nearly the same, the results are directly comparable between the closed and open well tests. Note also that the temperature difference is small between different flow rates for the closed well tests, indicating the advection outside the test well (sleeve only prevents water from entering the well) has a small impact on GFC temperatures.

Figure 7 demonstrates the relative roles of thermal conduction and advection during GFC heating tests. At lower Darcy velocities, the difference between the combined conduction and advection (Open 10 hour) and the conduction (Closed 10 Hour) is small, indicating the amount of heat removed by advection is small relative to thermal conduction. As Darcy velocities increase, the difference between the two curves increases, indicating the amount of heat removed by advection becomes relatively larger.

The initial results of closed versus open well test tests are important for cases that do not have a homogenous thermal conductivity profile near the well. If a location has a higher thermal conduction, it may provide a false signal for higher groundwater flux by giving a lower temperature response when the thermal conductivity is inappropriately assumed homogeneous (Fig.8). The closed versus open well test approach can provide an effective diagnostic for identifying this potential problem. As shown in Fig. 7, if the temperature difference is not caused by advection, the temperature response will be very similar between the open and closed well tests.

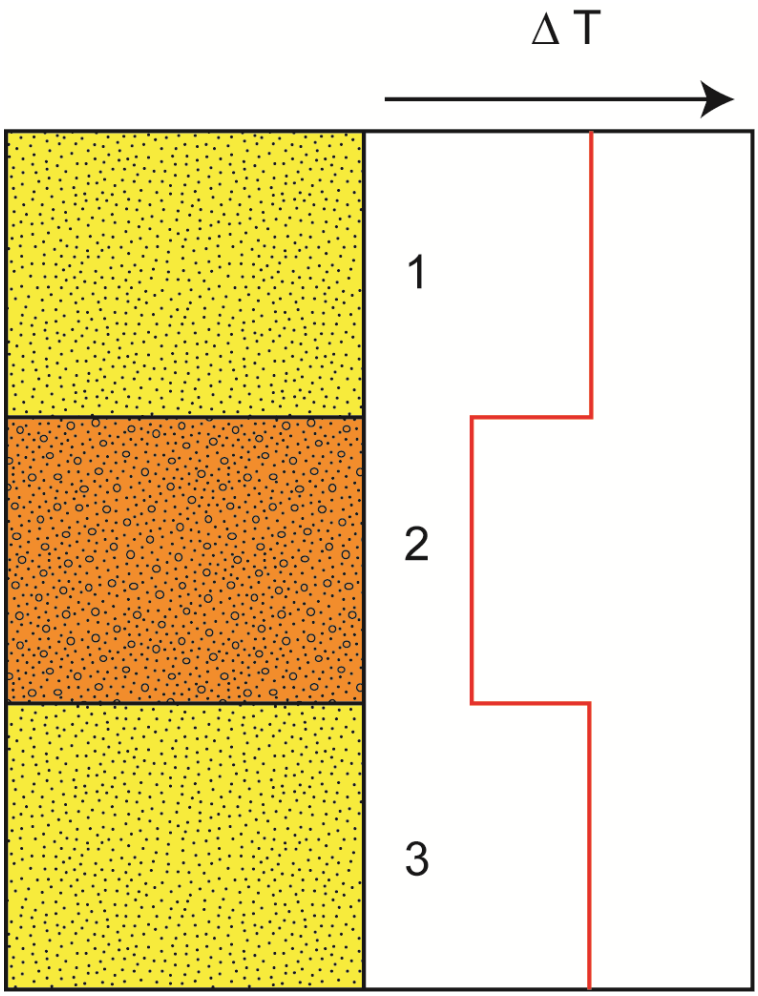

Figure 8. Cartoon of the effect of different thermal conductivities on temperature response. Layers 1 and 3 have the same thermal conductivity whereas layer 2 is higher. The red line represents an open well heating test. Assuming homogenous thermal conductivity, the temperature response at layer 2 could be mistakenly attributed to a higher flux.

Conclusions and Future Work

Using a laboratory sandbox setting, the relationship between the temperature response of GFC and groundwater flux has been obtained in a homogenous sandbox. Results confirmed that lower groundwater flux values produced higher temperature during GFC heating tests, and vice versa. The 5 hour and 10 hour curves produced from the experiments show a linear relationship that could be potentially used to

quantify groundwater flux values from temperature data in applicable field conditions. A new sleeved GFC probe method shows promise as a means to resolve two major heat transport mechanisms, thermal advection and conduction, during the GFC heating tests.

Improvements to the box and probe can help alleviate some of the issues that are present in the current data. The largest concern is the inability to control the climate in the current lab, hence the need to perform background temperature corrections. Having climate control would better simulate groundwater temperature under actual aquifer conditions and remove uncertainty in the data caused by large background temperature shifts. The second concern is the combination of the current sand parameters and well slot size. The initial packing of the sand did not provide enough compaction to lower the hydraulic conductivity to a more reasonable value (< 100 m/d), and the small slot size for the well was chosen for future runs that would use smaller grained material. However, the current combination of the small well opening and large hydraulic conductivity of the sand in the box may be causing flow to divert away from the well instead of toward it, thus reducing the sensitivity of GFC probe to flux variations. This concern is mainly for the lower Darcy velocities, and may be the reason for some of the temperature responses of 0.25 m/d runs not showing a significant difference from those for the no flow runs. An increased well slot size is recommended along with a more thorough compaction method for the sand in future sandbox modification.

As discussed earlier, tests at lower Darcy velocities (< 0.25 m/d) need to be performed to better understand the relationship between advection and thermal conduction as thermal conduction becomes more dominant. More 10 hour open tests

need to be performed to confirm that longer periods improve temperature signals and the relationship between temperature response and groundwater flux.

References

Anderson, M. P. (2005), Heat as a ground water tracer, *Ground Water*, 43(6), 951–968

Ballard, S. (1996), The in situ permeable flow sensor: a ground-water flow velocity meter, *Ground Water*, 34(2), doi:10.1111/j.1745-6584.1996.tb01883.x.

Barth, G.R., M.C. Hill, T.H. Illanasekare, and H. Rajaram (2001), Predictive modeling of flow and transport in a two-dimensional intermediate-scale, heterogeneous porous medium, *Water Resources Research* 37(10), 2503–2512.

Bayless, E. R., W. A. Mandell, and J. R. Urisc (2011), Accuracy of flowmeters measuring horizontal groundwater flow in an unconsolidated aquifer simulator, *Ground Water Monit. R*., 31(2), doi:10.1111/j1745-6592.2010.01324.x.

Becker, M. and A. Hawkins (2012), Measurement of the spatial distribution of heat exchange in a geothermal analog bedrock site using fiber optic distributed temperature sensing, In *3 Workshop on Geothermal Reservoir Engineering Stanford University*, Stanford, California, January 30 - February 1, 2012 SGP-TR-194, SGP-TR-194. Palo Alto, California: Stanford University.

Bowen, I. R., Devlin, J.F. and Schillig, P. C. (2012), Design and Testing of a Convenient Benchtop Sandbox for Controlled Flow Experiments, Groundwater *Monitoring & Remediation*, 32, 87–91. doi: 10.1111/j.1745-6592.2012.01400.x

Close, M., Bright, J., Wang, F., Pang, L. and Manning, M. (2008), Key Features of Artificial Aquifers for Use in Modeling Contaminant Transport, *Groundwater*, 46: 814-828. doi: 10.1111/j.1745-6584.2008.00474.x

Dagan, G. (1989), Flow and Transport in Porous Formations, Springer-Verlag, New York, 465 p.

Danquigny, C., P. Ackerer, and J.P. Carlier (2004), Laboratory tracer tests on three-dimensional reconstructed heterogeneous porous media, *Journal of Hydrology* 294(1-3), 196–212.

Fernàndez-Garcia, D., T. H. Illangasekare, and H. Rajaram (2004), Conservative and sorptive forced-gradient and uniform flow tracer tests in a three-dimensional laboratory test aquifer, *Water Resour. Res*., 40, W10103, doi:10.1029/2004WR003112.

Fetter, C.W. (2001), Applied Hydrogeology, 4th ed. Columbus, OH: Merrill Publishing Co.

Förster, A., Schrötter, J., Merriam, D.F. & Blackwell, D. (1997). Application of optical-fiber temperature logging—An example in a sedimentary environment, *Geophysics*, 62(4),1107-1113, ISSN 0016-8033

Freeze, R.A., and J.A. Cherry (1979), Groundwater, Englewood, CA: Prentice-Hall, Inc.

Freifeld, B. M., S. Finsterle, T. C. Onstott, P. Toole, and L. M. Pratt (2008), Ground surface temperature reconstructions: Using in situ estimates for thermal conductivity acquired with a fiber-optic distributed thermal perturbation sensor, *Geophys. Res*. *Lett.*, 35, L14309, doi:10.1029/2008GL034762.

Guaraglia, D.O., Mayosky, M.A., Pousa, J.L., Kruse, E.E. (2008), Numerical and experimental study of a thermal probe for measuring groundwater velocity, *Rev. Sci. Insturm.* 79, 15102.

Hatfield, K., M. Annable, J. Cho, P. S. C. Rao, and H. Klammler (2004), A direct passive method for measuring water and contaminant fluxes in porous media, *J. Contam. Hydrol.*, 75(3), doi:10.1016/j.jconhyd.2004.06.005.

Hausner, M. B., F. Suarez, K. E. Glander, N. V. D. Giesen, J. S. Selker, and S. W. Tyler (2011), Calibrating single-ended fiber-optic raman spectra distributed temperature sensing data, *Sensors*, 11(10),859–10,879, doi:10.3390/s111110859.

Hurtig, E., Schrötter, J., Großwig, S., Kühn, K., Harjes, B., Wieferig, W., and Orrell, R.P. (1993), Borehole temperature measurements using distributed fibre optic sensing; *Scientific Drilling*, 3 (6), p. 283-286.

Jose, S. C., M. A. Rahman, and O. A. Cirpka (2004), Large-scale sandbox experiment on longitudinal effective dispersion in heterogeneous porous media, *Water Resour. Res.*, 40, W12415, doi:10.1029/2004WR003363.

Kelly, S. E., and L. C. Murdoch (2003), Measuring the hydraulic conductivity of shallow submerged sediments, *Ground Water*, 41(4),431–439.

Kerfoot, W.B. (1988), Monitoring well construction and recommended procedures for direct ground-water flow measurements using a heat-pulsing flowmeter, *Ground-Water Contamination—Field Methods (Special Technical Publication 963)*, ed. A.G. Collins and A.I. Johnson, 146–161. Philadelphia, PA: American Society for Testing and Materials.

Labaky, W., J. F. Devlin, and R. W. Gillham (2009), Field comparison of the point velocity probe with other groundwater velocity measurement methods, *Water Resour. Res.*, 45, W00D30, doi:10.1029/2008WR007066.

Labaky, W., J. F. Devlin, and R. W. Gillham (2007), Probe for measuring groundwater velocity at the centimeter scale, *Environ. Sci. Technol.,* 41(24), 8453–8458, doi:10.1021/es0716047.

Leaf, A. T., D. J. Hart, and J. M. Bahr (2012), Active thermal tracer tests for improved hydrostratigraphic characterization, *Ground Water*, 50(5), doi:10.1111/j.1745-6584.2012.00913.x.

Liu, G., S. Knobbe, and J. Butler (2013), Resolving centimeter-scale flows in aquifers and their hydrostratigraphic controls, *Geophys. Res. Lett*., 40, 1098–1103, doi:10.1002/grl.50282.

Lowry, C. S., J. F. Walker, R. J. Hunt, and M. P. Anderson (2007), Identifying spatial variability of groundwater discharge in a wetland stream using a distributed temperature sensor, *Water Resour. Res.*, 43, W10408, doi:10.1029/2007WR006145.

Macfarlane, A., A. Forster, D. Merriam, J. Schr otter, and J. Healey (2002), Monitoring artificially stimulated fluid movement in the Cretaceous Dakota aquifer, western Kansas, *Hydrogeol. J.*, 10(6), 662–673, doi:10.1007/s10040-002-0223-7.

Pedler, W.H., R.E. Crowder, J.M. Seracuse, N.J. Myers, J. Daniel, and L. Haines (1995), Vertical profiling of aquifer flow characteristics and water quality parameters using HydroPhysical Logging, *Symposium on the Application of Geophysics to Engineering and Environmental Problems,* 8: 311.

Rau, G. C., M. S. Andersen, A. M. McCallum, H. Roshan, and R. I. Acworth (2014), Heat as a tracer to quantify water flow in near-surface sediments, *Earth Sci. Rev.*, 129, 40–58.

Schuetz, T., and M. Weiler (2011), Quantification of localized groundwater inflow into streams using ground-based infrared thermography, *Geophys. Res. Lett.*, 38, L03401, doi:10.1029/2010GL046198.

Selker, J. S., et al. (2006), Distributed fiber-optic temperature sensing for hydrologic systems, *Water Resour. Res.*, 42, W12202, doi:10.1029/ 2006WR005326.

Silliman, S.E., L. Zheng, and P. Conwell (1998), The use of laboratory experiments for the study of conservative solute transport in heterogeneous porous media, *Hydrogeology Journal* 6(1), 166–177.

Suárez, F., Hausner, M.B., Dozier, J., Selker, J.S., Tyler, S.W., (2011), Heat Transfer in the Environment : Development and Use of Fiber-Optic Distributed Temperature Sensing, DOI: 10.5772/19474 in: Developments in Heat Transfer. InTech.

Suthersan, S., C. Divine, J. Quinnan, and E. Nichols (2010), Flux-informed remediation decision making, *Ground Water Monit. R.,* 30(1), doi:10.1111/j.1745-6592.2009.01274.x.

Tsang, C.F., P. Hufschmied, and F.V. Hale (1990), Determination of fracture inflow parameters with a borehole fluid conductivity logging method. *Water Resources Research* 26, 561–578.

Tyler, S. W., J. S. Selker, M. B. Hausner, C. E. Hatch, T. Torgersen, C. E. Thodal, and S. G. Schladow (2009), Environmental temperature sensing using Raman spectra DTS fiber-optic methods, *Water Resour. Res.,* 45, W00D23, doi:10.1029/2008WR007052.

van de Giesen, N., S. C. Steele-Dunne, J. Jansen, O. Hoes, M. B. Hausner, S. W. Tyler, and J. S. Selker (2012), Double-ended calibration of fiber-optic Raman spectra distributed temperature sensing data, *Sensors*, 12, doi:10.3390/s120505471.

Vogt, T., P. Schneider, L. Hahn-Woernle, and O. A. Cirpka (2010), Estimation of seepage rates 294 in a losing stream by means of fiber-optic high-resolution vertical temperature profiling, *J. Hydrol.,* 380(1-2), doi:10.1016/j.jhydrol.2009.10.033.

Westhoff, M. C., H. H. G. Savenije,W. M. J. Luxemburg, G. S. Stelling, N. C. van de Giesen, J. S. Selker, L. Pfister, and S. Uhlenbrook (2007), A distributed stream

temperature model using high resolution temperature observations, *Hydrol. Earth Syst. Sci.*, 11, 1469– 1480.

Wilson, J.T., W.A. Mandell, F.L. Paillet, E.R. Bayless, R.T. Hanson, P.M. Kearl, W.B. Kerfoot, M.W. Newhouse, and W.H. Pedler (2001), An evaluation of borehole flowmeters used to measure horizontal ground-water flow in limestones of Indiana, Kentucky, and Tennessee, 1999, U.S. Geological Survey Water-Resources Investigations Report 01–4139.

Appendix A

Flow and Heating Tests Data

I.D.	Active Heating (Hours)	Screen (Open or Closed)	Date	Delta T (°C)	RMSE (°C)	Average Darcy Velocity (m/d)	Standard Deviation (m/d)
1	5	Open	11/8/2013	1.82	0.0515	0.000	0.0000
2	5	Open	11/10/2013	1.62	0.0442	0.268	0.0046
3	5	Open	11/11/2013	1.52	0.0413	0.373	0.0037
4	5	Open	11/13/2013	1.55	0.0457	0.507	0.0035
5	5	Open	11/15/2013	1.39	0.0446	0.641	0.0053
6	5	Open	11/18/2013	1.17	0.0436	0.768	0.0037
7	5	Open	11/19/2013	1.12	0.0430	0.895	0.0053
8	5	Open	11/20/2013	1.13	0.0429	1.010	0.0047
9	5	Open	11/22/2013	0.98	0.0417	1.280	0.0091
10	5	Open	11/23/2013	0.96	0.0456	1.158	0.0076
11	5	Open	11/24/2013	1.30	0.0454	0.762	0.0056
12	5	Open	11/26/2013	1.84	0.0444	0.000	0.0000
13	5	Open	11/28/2013	0.97	0.0449	1.282	0.0120
14	5	Open	11/30/2013	1.06	0.0528	1.153	0.0088
15	5	Open	12/1/2013	1.22	0.0424	0.992	0.0058
16	5	Open	12/2/2013	1.32	0.0456	0.881	0.0061
17	5	Open	12/3/2013	1.43	0.0520	0.761	0.0054
18	5	Open	12/4/2013	1.30	0.0453	0.626	0.0072
19	5	Open	12/5/2013	1.51	0.0449	0.509	0.0055
20	5	Open	12/6/2013	1.63	0.0470	0.373	0.0048
21	5	Open	12/8/2013	1.84	0.0538	0.254	0.0053
22	5	Open	1/15/2014	1.17	0.0557	0.897	0.0083
23	5	Open	1/16/2014	1.26	0.0495	0.750	0.0128
24	5	Open	1/17/2014	1.44	0.0486	0.627	0.0200
25	5	Open	1/21/2014	1.86	0.0453	0.000	0.0000
26	5	Open	1/23/2014	1.77	0.0428	0.263	0.0143
27	5	Open	1/28/2014	1.57	0.0616	0.509	0.0244
28	5	Open	1/29/2014	1.32	0.0460	0.768	0.0142
29	10	Open	1/17/2014	1.57	0.0486	0.627	0.0196
30	10	Open	1/21/2014	2.06	0.0453	0.000	0.0000
31	10	Open	1/23/2014	1.97	0.0428	0.263	0.0140
32	10	Open	1/28/2014	1.73	0.0616	0.509	0.0240
33	10	Open	1/29/2014	1.47	0.0460	0.768	0.0181
34	10	Closed	5/19/2014	1.79	0.0459	0.000	0.0000
35	10	Closed	5/21/2014	1.86	0.0489	0.000	0.0279

I.D.	Active Heating (Hours)	Screen (Open or Closed)	Date	Delta T (°C)	RMSE (°C)	Average Darcy Velocity (m/d)	Standard Deviation (m/d)
36	10	Closed	5/23/2014	1.84	0.0464	0.252	0.0169
37	10	Closed	5/26/2014	1.85	0.0456	0.252	0.0000
38	10	Closed	5/28/2014	1.88	0.0457	0.000	0.0276
39	10	Closed	5/30/2014	1.82	0.0456	0.000	0.0226
40	10	Closed	6/2/2014	1.86	0.0445	0.000	0.0000
41	10	Closed	6/4/2014	1.94	0.0492	0.276	0.0115
42	10	Closed	6/6/2014	1.70	0.0486	0.506	0.0051
43	10	Closed	6/9/2014	1.69	0.0421	0.506	0.0000
44	10	Closed	6/11/2014	1.72	0.0448	0.399	0.0073
45	10	Closed	6/13/2014	1.69	0.0473	0.728	0.0397